

# Rapid formation of intense haze episodes via aerosol-boundary layer feedback in Beijing

Yonghong Wang<sup>1,2</sup>, Miao Yu<sup>3</sup>, Yuesi Wang<sup>1,6</sup>, Guiqian Tang<sup>1</sup>, Tao Song<sup>1</sup>, Putian Zhou<sup>2</sup>, Zirui Liu<sup>1</sup>,  
Bo Hu<sup>1</sup>, Dongsheng Ji<sup>1</sup>, Lili Wang<sup>1</sup>, Xiaowan Zhu<sup>1</sup>, Chao Yan<sup>2</sup>, Mikael Ehn<sup>2</sup>, Wenkang  
Gao<sup>1</sup>, Yuepeng Pan<sup>1</sup>, Jinyuan Xin<sup>1</sup>, Yang Sun<sup>1</sup>, Veli-Matti Kerminen<sup>2</sup>, Markku Kulmala<sup>2,4,5</sup> and  
Tuukka Petäjä<sup>2,4,5</sup>

<sup>1</sup>State Key Laboratory of Atmospheric Boundary Layer Physics and Atmospheric Chemistry  
(LAPC), Institute of Atmospheric Physics, Chinese Academy of Sciences, Beijing 100029, China

<sup>2</sup>Institute for Atmospheric and Earth System Research / Physics, Faculty of Science, P.O.Box 64,  
00014 University of Helsinki, Helsinki, Finland

<sup>3</sup>Institute of Urban Meteorology, China Meteorological Administration, Beijing, China

<sup>4</sup>Joint international research Laboratory of Atmospheric and Earth System sciences (JirLATEST),  
Nanjing University, Nanjing, China

<sup>5</sup>Aerosol and Haze Laboratory, Beijing Advanced Innovation Center for Soft Matter Science and  
Engineering, Beijing University of Chemical Technology (BUCT), Beijing, China

<sup>6</sup>Centre for Excellence in Atmospheric Urban Environment, Institute of Urban Environment,  
Chinese Academy of Science, Xiamen, Fujian 361021, China

Corresponding authors: Yuesi Wang and Markku Kulmala

E-mail: [wys@mail.iap.ac.cn](mailto:wys@mail.iap.ac.cn); [markku.kulmala@helsinki.fi](mailto:markku.kulmala@helsinki.fi)

Revised to: Atmospheric Chemistry and Physics

**Keywords:** PM<sub>2.5</sub>, Mixing layer height, Turbulent kinetic energy, vertical measurement, model,  
feedback

## Abstract

Although much efforts have been put on studying air pollution, our knowledge on the mechanisms of frequently occurred intense haze episodes in China is still limited. In this study, using three years of measurements of air pollutants at three different height levels on a 325-meter Beijing meteorology tower, we found that a positive aerosol-boundary layer feedback mechanism existed at three vertical observation heights during intense haze polluted periods within the mixing layer. This feedback was characterized by a higher loading of  $PM_{2.5}$  with a shallower mixing layer. Modeling results indicated that the presence of  $PM_{2.5}$  within boundary layer lead to reduced surface temperature, relative humidity and mixing layer height during an intensive haze episode. Measurements showed that the aerosol-boundary layer feedback was related to the decrease of solar radiation, turbulent kinetic energy and thereby suppression of the mixing layer. The feedback mechanism can explain the rapid formation of intense haze episodes to some extent, and we suggest that the detailed feedback mechanism warrant further investigation both from model simulations and field observations.

## 1. Introduction

With the rapid economic growth and urbanization, an increasing frequency of haze episodes along with the air pollution has become of great concern in China during the last decade (Cao et al., 2016; Huang et al., 2014; Kulmala, 2015; Wang et al., 2014; Wang et al., 2015). For example, during December 2016 a series of intense haze episodes took place in Eastern China, characterized by surface  $PM_{2.5}$  concentrations exceeding  $500 \mu g m^{-3}$  in several measurement sites in Beijing and its surrounding sites ([http://www.mep.gov.cn/gkml/hbb/qt/201701/t20170102\\_393745.htm](http://www.mep.gov.cn/gkml/hbb/qt/201701/t20170102_393745.htm)). Severe air pollution has serious effects on human health. A recent study reported that the particulate matter has significantly decreased the life span of residents as many as 5.5 years in Northern China (Chen et al, 2013). In a global scale, the air pollution was estimated to cause over 3 million premature deaths every year (Lelieveld et al., 2015).

Increased emissions from fossil fuel combustion due to vehicle traffic, industrial activities and power generation, along with exceptionally strong secondary aerosol formation, were thought to be responsible for these haze episodes (Cheng et al., 2016; Huang et al., 2014; Pan et al., 2016; Petäjä et al., 2016; G Wang et al., 2016a; Zhang et al., 2015; Zhao et al., 2013). Meanwhile, the formation of intense haze episodes was considered to be affected by meteorological conditions (Wang et al.,

2014; Quan et al., 2013; Wang et al., 2016b; Zheng et al., 2016). For example, the mixing layer height is a key parameter that constrains the dilution of surface air pollution, and the development of mixing layer is highly related to the amount of solar radiation absorbed by the air and reaching the surface (Ding et al., 2016; Stull, 1988; Sun et al., 2013; Tang et al., 2016; Wilcox et al., 2016). By using filed measurements combined with model simulation, a positive feedback between aerosol pollution, relative humidity and boundary layer was found to be important in aerosol production, accumulation and severe haze formation in Beijing (Liu et al., 2018). Wang et al. (2018) found that PBL schemes in their atmospheric chemistry models are not sufficient to describe the explosive growth of PM<sub>2.5</sub> concentration in Beijing-Tianjin-Hebei region due to absence of an online calculation of aerosol-radiation feedback, and/or a deficient description of extremely weak turbulent diffusion.

In this study, using unique measurements on the Beijing 325-meter-high meteorology tower, we show clear relationship between mixing layer height and turbulent kinetic energy at the 140-m observation platform. We also present direct evidence on the feedback that relates the decreasing mixed layer height with increasing particulate matter concentrations, and this feedback is critical to the formation of intense haze episodes in Beijing.

## 2. Methods

### 2.1 Calculation of mixing layer height with ceilometer

The ceilometer was deployed in the yard of IAP (Institute of atmospheric physics, Chinese academy of science), with a horizontal distance around tens of meters from the 325-m meteorology tower. The mixing layer height was measured with the enhanced single-lens ceilometers from July of 2009 to August of 2012 (CL 31, Vaisala, Finland), which utilized the strobe laser lidar technique (910 nm) to measure the attenuated backscattering coefficient profiles. Detection range of the CL31 is 7.6 km with the report period of 2-120 s. Detail information can be found in previous studies (Tang et al., 2016). Since the distribution of particle concentrations is uniform in the mixing layer and has significant differences between the mixing layer and free atmosphere, the height at where a sudden change exists in the attenuated backscattering coefficient profile indicates the top of the mixing layer height. The Vaisala software product BL-VIEW was used to determine the mixing layer height by finding the position with the maximum negative gradient ( $-d\beta/dx$ ) in the attenuated

backscattering coefficient profiles as the top of the mixing layer (Münkel et al., 2007).

## 2.2 Measurements of energy flux at the 325-m Beijing meteorology tower

The turbulent fluxes of sensible heat ( $Q_H$ ), latent heat ( $Q_E$ ) and the turbulence kinetic energy (TKE) were measured at the 140-m level using eddy covariance technique from July of 2009 to August of 2012. The raw data (10 Hz) of wind components ( $u$ ,  $v$  and  $w$ ) and sonic temperature ( $T_s$ ) recorded with three-dimensional sonic anemometers (Model CSAT3, Campbell Scientific Inc., Logan, Utah, USA) and of water vapor concentrations ( $q$ ) with open-path infrared gas analyzers (Model LI-7500, LiCor Inc., Lincoln, Nebraska, USA). The fluxes of heat ( $Q$ ) were calculated as the covariance between the instantaneous deviation or fluctuations of vertical velocity ( $w'_i$ ) and their respective scalar ( $s'_i$ ) averaged over a time interval of 30 min:

$$Q = \overline{w's'} = \frac{1}{N} \sum_{i=1}^N w'_i s'_i$$

Where the over-bar denotes a time average,  $N$  is the number of samples during the averaging time and the fluctuations are the differences between the instantaneous readings and their respective means. The TKE were calculated as follows (stull,1988):

$$\frac{TKE}{m} = \frac{1}{2} (\overline{u'^2} + \overline{v'^2} + \overline{w'^2}) = \bar{e}$$

where  $m$  is the mass (kg),  $e$  is the TKE per unit mass ( $m^2 s^{-1}$ ). A more detailed description of the calculation and post processing of flux is provided elsewhere (Song et al., 2013).

## 2.3 Measurements of $PM_{2.5}$ concentration and gases at the 325-m Beijing meteorology tower.

The mass concentration of  $PM_{2.5}$  at 8-m, 120-m and 280-m observation platforms were measured with three TEOM RP1400 simultaneously from July of 2009 to August of 2012. (Thermo Scientific, <http://www.thermoscientific.com>). The resolution and precision of the instrument for one-hour measurements were  $0.1 \mu g m^{-3}$  and  $\pm 1.5 \mu g m^{-3}$ , respectively. The filters were exchanged when the loading rates were approximately 40%. The flow rate was monitored and calibrated monthly. The volume mixing ratios of ozone and  $NO_x$  were measured with 49i and 42i (Thermal Environment Instruments (TEI) Inc.), respectively (Wang et al., 2014).

## 2.4 Experiment design

The model used in this study is the Weather Research and Forecasting (WRF) model (ARW, version 3.8.1; Skamarock et al. 2008). The simulation domain was centered in Beijing (39.0°N, 116.0°E)

and implemented with one-nested grids with a resolutions of 1 km. The number of grid cells was  $460 \times 403$  for the domain in the east-west and south-north directions. The model run was initialized at 00:00 UTC (or 08:00 LST) 16 Nov 2010 and integrated for 131 h until 10:00 UTC 21 Nov 2010, including 48 h for spin-up. The initial conditions of the model and its outermost lateral boundary conditions, as well as the soil moisture field, were taken from National Centers for Environmental Prediction/National Center for Atmospheric Research Reanalysis data (resolution:  $1^\circ \times 1^\circ$ ). The model physics schemes used include: Thompson microphysical parameterization (Thompson et al., 2004); BouLac boundary-layer parameterization (Bougeault and Lacarrere 1989); RRTMG (Iacono et al., 2008) radiation Scheme; The Building Effect Parameterization (BEP) and the Building Energy Model (BEM) schemes implemented in WRF that can more accurately describe three-dimensional urban land surface features and processes, including anthropogenic heat from buildings (Martilli et al., 2002; Salamanca and Martilli, 2010). The control and test experiment were performed separately to investigate impact of aerosol direct radiative forcing on surface temperature, relative humidity and development of boundary layer height. The control run (CTL) used the RRTMG radiation scheme which ignored the direct radiation effects of aerosols input. In sensitivity test experiment, we add the aerosol input in RRTMG scheme using Tegen climatology and urban type aerosols during the sensitive test.

## 2.5 Other supporting measurements

Total solar radiation was measured with a direct radiometer (TBQ-2, Junzhou, China). Direct radiation was measured with a direct radiometer (TBS-2, Junzhou, China). UV radiation in the range of 220-400 nm was measured using CUV3 radiometer (USA). The estimated experiment error for the three instruments are 3%, 1% and 2%, respectively. The original data were obtained at one-minute intervals and the hourly average values were used in this study. The chemical composition of organic, sulphate, nitrate, ammonium and chloride in non-refractory submicron aerosol were measured during several campaigns with an Aerodyne High-Resolution Time-of-Flight Aerosol Mass Spectrometer from July of 2009 to August of 2012 (HR-ToF-AMS, Aerodyne Research Inc., Billerica, MA, USA). Detailed information about instrument, calibration and data process have been introduced by. All these measurements were conducted in the IAP station.

## 3 Results and Discussion

A typical intense haze episode occurred during the heating season in urban Beijing during 17 to 22 November 2010. This episode was associated with synoptic stagnation in the North China Plain

(Figure S1) and was characterized by low wind speeds and irregular wind direction (Figure 1). Several meteorological variables had distinct temporal patterns during different stages of pollution, including reduced solar radiation and increased relative humidity during the most intense presence of haze (Fig. 1). The temporal patterns of PM<sub>2.5</sub> concentrations were very similar at the two lower measurements heights (8 m and 120 m, Fig. 1d), even though the concentration was clearly the highest close to the surface. The PM<sub>2.5</sub> concentration measured at 280 m behaved in a different way, especially during the most intense period of the haze when the mixed layer height was very low (Fig. 1e). The decoupling of the 280-m platform from the other two lower ones at low mixed layer heights is apparent in our 3-year measurement data set, especially when comparing O<sub>3</sub> and NO<sub>x</sub> concentrations between the three measurement platforms (Figs. S2 and S5). During the haze period, the maximum PM<sub>2.5</sub> concentrations at 8, 120 and 280 m were 505, 267 and 339  $\mu\text{g m}^{-3}$ , respectively. The higher maximum concentration at 280 m compared with 120 m can be ascribed to the transport of pollutants from surrounding regions of Hebei and Tianjin Provinces typical for polluted periods (Sun et al., 2013). The mixing layer height varied from 130 m to 1640 m during the haze episode, ranging between about 200 and 500 m during the most intense period of the haze period on 18 November 2010 (Fig. 1e). The TKE was quite low during this intensive haze episode from 18 November to 21 November, with an average value around 0.3  $\text{m}^2 \text{s}^{-2}$ . However, the TKE increased significant on morning of 21 November as surface wind increased from 1.2 m/s to around 6 m/s, which was possible due to the movement of cold front as shown in Figure S1.

The vertical distribution of attenuated backscatter density obtained from ceilometer measurements indicate vertical mixing conditions accompanied with an inversion layer and high relative humidity in the surface as shown in Figure 2. The strong inversion and high relative humidity occurred on morning of 18 November 2010, with a lapse rate of 2K / 100 m, relative humidity of 78% and north-direction wind speed of around 2 m / s detected by the vertical sounding. The turbulent kinetic energy at 140 m was reduced to around 0.1~0.7  $\text{m}^2/\text{s}^2$  due to decreased solar radiation, as presented in Figure1(a). In this manner, the development of a mixing layer was significantly suppressed during the intense haze episode.

In order to demonstrate how the PM<sub>2.5</sub> modifies the surface temperature, relative humidity and development of the mixing layer height. we performed two numerical simulation experiments, using the WRF model as a tool. We took the measurements during the intensive haze episode shown in Figure 1 as an example. As shown in Figure 3(a), the variation of temperature and relative humidity

showed pronounced daily variations, with higher and lower values, respectively, during daytime in both test and control experiment. However, the presence of aerosol in the test experiment clearly showed decreased surface temperature and increased relative humidity. The presence of aerosol reduces downward radiation reaching the surface, as a result of which the surface temperature and sensitive heat flux decrease, and the development of mixing layer height is suppressed (Li et al., 2017a, 2017b; Miao et al., 2016). Statistical results showed that the average relative humidity, surface temperature and mixing layer height were  $8.2 \pm 3.4$  °C,  $40.5 \pm 11.6\%$  and  $377.7 \pm 499$  m, respectively, without the consideration of aerosol direct radiative forcing, whereas the consideration of aerosol directive radiative forcing changed these values to  $7.1 \pm 3.1$  °C,  $40.6 \pm 11.7\%$  and  $326.7 \pm 470.1$  m, respectively. Our model results clearly demonstrate the pronounced role of aerosol particles in reducing the mixing layer height during this haze pollution episode.

In order to further illustrate how the mixing layer height modifies  $PM_{2.5}$  concentrations, we used three years of simultaneous winter-time air pollutant measurements in the Beijing. We divided the observed  $PM_{2.5}$  concentrations into highly-polluted and less-polluted conditions using a threshold value of  $75 \mu g m^{-3}$  for  $PM_{2.5}$  to distinguish between these conditions. This is consistent with Chinese Environment Protection Bureau definition of a haze pollution events. With this threshold value, we found that 31% and 69% of total measurement time corresponded to highly-polluted and less-polluted conditions, respectively. We plotted the  $PM_{2.5}$  data as a function of the mixing layer height at the three observation heights (8 m, 120 m and 280 m) during both highly-polluted and less-polluted conditions and fitted an exponential curve to these data based on best fitting (Figure. 4). The  $PM_{2.5}$  concentration has a clear anti-correlation with the mixing layer height during the intense haze episodes. At all the measurement heights, the  $PM_{2.5}$  concentration increased as the mixing layer height decreased, and this pattern was very strong under polluted conditions (Figure. 4). We also tested the reciprocal fitting function for the data (Figure S8). It overestimated the  $PM_{2.5}$  concentration when the mixing layer height was very low, as compared to the exponential fitting function (Figure. 4). This also indicates that a much higher  $PM_{2.5}$  concentration is needed in order to obtain a very low mixing layer height without the positive feedback. This can also be supported by the root-mean-square error (RMSE) of these two fitting methods. The RMSE of the exponential fitting is much smaller than the reciprocal fitting in any case (Table. S1).

It is worth noting that the increase was mainly from the  $PM_{1-2.5}$  fraction that increased from 42% to 65% as mixing layer height decreased from more than 1400 m to lower than 300 m (Figure S4). A

major portion of particulate mass between 1 and 2.5  $\mu\text{m}$  originates from secondary aerosol formation processes in urban air (Wang et al., 2014; Zhang et al., 2015). As shown in Figure S7, the concentration of NR-PM<sub>1</sub> increased significantly from 12.1  $\mu\text{g m}^{-3}$  to 56.4  $\mu\text{g m}^{-3}$  with the variation of MLH decreased from more than 1400 m to less than 200 m. The reduction in solar radiation reaching the surface due to fine particle matter reduces the turbulent kinetic energy and the development of mixing layer, as shown in Figure.5. An exponential function between the turbulent kinetic energy at 140 m and mixing layer height was fitted., Based on this fit, the MLH roughly be doubles from about 400 m to 800 m when TKE increases from 0.1  $\text{m}^2 \text{s}^{-2}$  to 1  $\text{m}^2 \text{s}^{-2}$ . These are typical values of MLH during polluted conditions in Beijing.

The reduced sensible heat and TKE due to aerosol particles reduces the entrainment of relatively dry air into mixing layer from above, which makes the air more humid within the mixing layer. This, together with the decreased surface temperature increases the relative humidity (Li et al., 2017b). The increased relative humidity enhances the aerosol water uptake and promotes the formation of secondary organic and inorganic aerosol via aqueous phase reactions (Liu et al., 2018; Wang et al., 2019), .enhancing light scattering and causing further reduction in the intensity of radiation reaching the surface. All these factors suppress the development of mixing layer height and enhance the accumulation of air pollutants within the mixing layer. We ascribe part of the observed increase in PM<sub>2.5</sub> and simultaneous decrease in the mixing layer height to the positive feedback associated with the particulate matter-mixing layer interaction (Petäjä et al. 2016, Ding et al. 2016), occurring at the same time as primary emissions and secondary formation are confined into a smaller volume of air. The feedback occurred at all the three observation platforms and appeared to be most intensive at 8 m. In an urban environment, NO<sub>x</sub> originates mainly from local anthropogenic emissions, whereas the sources of particulate matter include both primary emissions and secondary formation (Ehn et al., 2014; Jimenez et al., 2009; Zhang et al., 2015; Zhao et al., 2013). As shown in Figure S6, the median NO<sub>x</sub> concentration at 8 m was 250% higher under highly polluted conditions compared with less-polluted conditions as the mixing layer height decreased to 100-200 m, while the corresponding number for the PM<sub>2.5</sub> concentration was 360%.

The increase of the PM<sub>2.5</sub> concentration from less-polluted to highly-polluted conditions is mainly due to concentrated particulate matter caused by a decreased mixing layer height, which is accompanied by primary particle emissions, secondary aerosol formation and feedback from particulate matter-mixing layer height interactions. Compared with the increased amounts of NO<sub>x</sub>, we can roughly estimate that in maximum 110% of the increased PM<sub>2.5</sub> originates from secondary aerosol formation processes in this study. Of the remaining 250% of the PM<sub>2.5</sub> increase, potentially



a large fraction originates from particulate matter-mixing layer height interactions, but we cannot quantify this fraction at the moment.

#### 4 Conclusions

The development of mixing layer height in an urban city is affected by the intensity of incoming solar radiation. Our measurement at the 325-meter meteorology tower showed that the solar and ultraviolet radiation reaching the surface decrease considerably at increased pollution levels, which leads to a decreased TKE and, consequently, the suppression of mixing layer development. In turn, the shallowed mixing layer height further favors the enhancement of PM<sub>2.5</sub> concentration and its precursor gases from both direct emissions and secondary formation. This feedback mechanism may be an important reason for rapid increase of particulate matter from moderate-polluted conditions to periods of intense pollution in an urban atmosphere as the strength increased with the PM<sub>2.5</sub> concentration increased, although we cannot quantify the feedback amount exactly by observations currently. The particulate matter-mixing layer height feedback is probably a critical factor for the formation of intense haze periods from moderate-polluted periods in Beijing and other polluted cities.

#### Acknowledgements

This work was supported by the Ministry of Science and Technology of China (No: 2017YFC0210000), the National Research Program for key issues in air pollution control(DQGG0101) and Academy of Finland via Center of Excellence in Atmospheric Sciences.

#### Competing financial interests

The authors declare no competing financial interests.

#### Author contributions

M.K, T.P and Y.H.W, have the original idea of the research. Y.S.W, G.T, T.S, Z.L, B.H, L.W, X.Z,

D.J, W.G and Y.S conducted the longtime measurements and provided the data. M.Y conducted  
 model simulation. Y.H.W, G.T, S.T, P.Z, M.E, C.Y, V.K, T.P and M.K interpreted the data and  
 plotted the figures. Y.H.W wrote the manuscript, with contribution from all co-authors.

## References

- Bougeault, P., and P. Lacarrere. Parameterization of orography-induced turbulence in a mesobeta--  
 scale model. Monthly Weather Review 117, 1872-1890, 1989.
- Cao, C., X. Lee, S. Liu, N. Schultz, W. Xiao, M. Zhang, and L. Zhao, Urban heat islands in China  
 enhanced by haze pollution, Nature Communications, 7, 12509, doi:10.1038/ncomms12509, 2016.  
<http://www.nature.com/articles/ncomms12509#supplementary-information>.
- Cheng, Y., et al. Reactive nitrogen chemistry in aerosol water as a source of sulfate during haze  
 events in China, Science Advances, 2(12), doi:10.1126/sciadv.1601530, 2016.
- DeCarlo, P. F., Kimmel, J. R., Trimborn, A., Northway, M. J., Jayne, J. T., Aiken, A. C., Gonin, M.,  
 Fuhrer, K., Horvath, T., Docherty, K. S., Worsnop, D. R., and Jimenez, J. L.: Field-Deployable,  
 High-Resolution, Time-of-Flight Aerosol Mass Spectrometer, Analytical Chemistry, 78, 8281-8289,  
 10.1021/ac061249n, 2006.
- Ding, A. J., et al. Enhanced haze pollution by black carbon in megacities in China, Geophysical  
 Research Letters, 43(6), 2873-2879, doi:10.1002/2016gl067745.
- Ehn, M., et al. (2014), A large source of low-volatility secondary organic aerosol, Nature, 506(7489),  
 476-479, doi:10.1038/nature13032, 2016.
- Huang, R.-J., et al. High secondary aerosol contribution to particulate pollution during haze events  
 in China, Nature, 514(7521), 218-222, doi:10.1038/nature13774, 2014.  
[http://www.nature.com/nature/journal/v514/n7521/abs/nature13774.html#supplementary-](http://www.nature.com/nature/journal/v514/n7521/abs/nature13774.html#supplementary-information)  
[information](http://www.nature.com/nature/journal/v514/n7521/abs/nature13774.html#supplementary-information).
- Hu, B., Wang, Y., and Liu, G.: Relationship between net radiation and broadband solar radiation in

the Tibetan Plateau, *Advances in Atmospheric Sciences*, 29, 135-143, 10.1007/s00376-011-0221-6, 2012.

Jiandong, Wang., et al., Impact of aerosol–meteorology interactions on fine particle pollution during China’s severe haze episode in January 2013, *Environmental Research Letters*, 9(9), 094002, 2014.

Jimenez, J. L., et al., Evolution of Organic Aerosols in the Atmosphere, *Science*, 326(5959), 1525-1529, doi:10.1126/science.1180353, 2009.

Kulmala, M., China’s choking cocktail, *Nature*, 526, 497-499, 2015.

Lelieveld, J., J. S. Evans, M. Fnais, D. Giannadaki, and A. Pozzer, The contribution of outdoor air pollution sources to premature mortality on a global scale, *Nature*, 525(7569), 367-371, doi:10.1038/nature15371, 2015.

Iacono, M. J., Delamere, J. S., Mlawer, E. J., Shephard, M. W., Clough, S. A. and Collins, W. D.: Radiative forcing by long-lived greenhouse gases: Calculations with the AER radiative transfer models, *Journal of Geophysical Research Atmospheres*, 113(13), 2–9, doi:10.1029/2008JD009944, 2008.

Li, M., Wang, T., Xie, M., Zhuang, B., Li, S., Han, Y. and Chen, P.: Impacts of aerosol-radiation feedback on local air quality during a severe haze episode in Nanjing megacity, eastern China, *Tellus, Series B: Chemical and Physical Meteorology*, 69(1), 1–16, doi:10.1080/16000889.2017.1339548, 2017a.

Li, Z., Guo, J., Ding, A., Liao, H., Liu, J., Sun, Y., Wang, T., Xue, H., Zhang, H. and Zhu, B.: Aerosol and boundary-layer interactions and impact on air quality, *National Science Review*, 4(6), 810–833, doi:10.1093/nsr/nwx117, 2017b.

Liu, Q., Jia, X., Quan, J., Li, J., Li, X., Wu, Y., Chen, D., Wang, Z. and Liu, Y.: New positive feedback mechanism between boundary layer meteorology and secondary aerosol formation during severe haze events, *Scientific Reports*, 8(1), doi:10.1038/s41598-018-24366-3, 2018.

Martilli, A., Clappier, A. and Rotach, M. W.: An urban surface exchange parameterisation for mesoscale models, *Boundary-Layer Meteorology*, 104(2), 261–304, doi:10.1023/A:1016099921195, 2002.

Miao, Y., Liu, S., Zheng, Y. and Wang, S.: Modeling the feedback between aerosol and boundary layer processes: a case study in Beijing, China, *Environmental Science and Pollution Research*, 23(4), 3342–3357, doi:10.1007/s11356-015-5562-8, 2016.

Münkel, C., Eresmaa, N., Räsänen, J. and Karppinen, A.: Retrieval of mixing height and dust concentration with lidar ceilometer, , 124, 117–128, doi:10.1007/s10546-006-9103-3, 2007.

Salamanca, F. and Martilli, A.: A new Building Energy Model coupled with an Urban Canopy

Parameterization for urban climate simulations-part II. Validation with one dimension off-line simulations, *Theoretical and Applied Climatology*, 99(3–4), 345–356, doi:10.1007/s00704-009-0143-8, 2010.

Thompson, G., Rasmussen, R. M. and Manning, K.: Explicit forecasts of winter precipitation using an improved bulk microphysics scheme. Part I: Description and sensitivity analysis, *Monthly Weather Review*, 132(2), 519–542 [online] Available from: [http://journals.ametsoc.org/doi/full/10.1175/1520-0493\(2004\)132%3C0519:EFOWPU%3E2.0.CO%3B2](http://journals.ametsoc.org/doi/full/10.1175/1520-0493(2004)132%3C0519:EFOWPU%3E2.0.CO%3B2), 2004.

Wang, Y., Wang, Y., Wang, L., Petäjä, T., Zha, Q., Gong, C., Li, S., Pan, Y., Hu, B., Xin, J. and Kulmala, M.: Increased inorganic aerosol fraction contributes to air pollution and haze in China, *Atmos. Chem. Phys*, 19, 5881–5888, doi:10.5194/acp-19-5881-2019, 2019.

Wang, Y. H., Hu, B., Ji, D. S., Liu, Z. R., Tang, G. Q., Xin, J. Y., Zhang, H. X., Song, T., Wang, L. L., Gao, W. K., Wang, X. K. and Wang, Y. S.: Ozone weekend effects in the Beijing-Tianjin-Hebei metropolitan area, China, *Atmos. Chem. Phys*, 14, 2419–2429, doi:10.5194/acp-14-2419-2014, 2014.

Münkel, C., Eresmaa, N., Räsänen, J., and Karppinen, A.: Retrieval of mixing height and dust concentration with lidar ceilometer, *Boundary-Layer Meteorology*, 124, 117–128, 10.1007/s10546-006-9103-3, 2007.

Pan, Y., et al., Redefining the importance of nitrate during haze pollution to help optimize an emission control strategy, *Atmospheric Environment*, 141, 197–202, doi:<http://dx.doi.org/10.1016/j.atmosenv.2016.06.035>, 2016.

Petäjä, T., et al., Enhanced air pollution via aerosol-boundary layer feedback in China, *Scientific Reports*, 6, 18998, doi:10.1038/srep18998 <http://www.nature.com/articles/srep18998#supplementary-information>, 2016.

Quan, J., Y. Gao, Q. Zhang, X. Tie, J. Cao, S. Han, J. Meng, P. Chen, and D. Zhao, Evolution of planetary boundary layer under different weather conditions, and its impact on aerosol concentrations, *Particuology*, 11(1), 34–40, doi:<http://dx.doi.org/10.1016/j.partic.2012.04.005>, 2013.

Salamanca F, Martilli A. A new building energy model coupled with an urban canopy parameterization for urban climate simulations–part II, Validation with one dimension off-line simulations. *Theoretical and Applied Climatology*. 99: 345–356, 2010.

Skamarock WC, Klemp JB, Dudhia J, Gill DO, Barker D, Wang W, Powers, JG. A description of the advanced research WRF version 3. NCAR/TN-475+STR, 2008.

Song, T., Sun, Y., and Wang, Y.: Multilevel measurements of fluxes and turbulence over an urban landscape in Beijing, *Tellus B: Chemical and Physical Meteorology*, 65, 20421, 10.3402/tellusb.v65i0.20421, 2013.

Stull, R. B., *An Introduction to Boundary Layer Meteorology*, Kluwer Academic Publishers, Dordrecht, 1988.

Sun, Y., T. Song, G. Tang, and Y. Wang, The vertical distribution of PM<sub>2.5</sub> and boundary-layer structure during summer haze in Beijing, *Atmospheric Environment*, 74, 413-421, doi:<http://dx.doi.org/10.1016/j.atmosenv.2013.03.011>, 2013.

Tang, G., Zhang, J., Zhu, X., Song, T., Munkel, C., Hu, B., Schäfer, K., Liu, Z., Wang, L., Xin, J., Suppan, P., and Wang, Y.: Mixing layer height and its implications for air pollution over Beijing, China, *Atmos. Chem. Phys.*, 16, 2459-2475, 10.5194/acp-16-2459-2016, 2016.

Wang, H., Peng, Y., Zhang, X., Liu, H., Zhang, M., Che, H. and Cheng, Y.: Contributions to the explosive growth of PM<sub>2.5</sub> mass due to aerosol – radiation feedback and decrease in turbulent diffusion during a red alert heavy haze in Beijing – Tianjin – Hebei , China, , 17717–17733, 2018.

Zhang, R., G. Wang, S. Guo, M. L. Zamora, Q. Ying, Y. Lin, W. Wang, M. Hu, and Y. Wang, Formation of Urban Fine Particulate Matter, *Chemical Reviews*, 115(10), 3803-3855, doi:10.1021/acs.chemrev.5b00067, 2015.

Zhao, B., S. X. Wang, H. Liu, J. Y. Xu, K. Fu, Z. Klimont, J. M. Hao, K. B. He, J. Cofala, and M. Amann, NO<sub>x</sub> emissions in China: historical trends and future perspectives, *Atmos. Chem. Phys.*, 13(19), 9869-9897, doi:10.5194/acp-13-9869-2013, 2013.

Zheng, G., F. Duan, Y. Ma, Q. Zhang, T. Huang, T. Kimoto, Y. Cheng, H. Su, and K. He, Episode-Based Evolution Pattern Analysis of Haze Pollution: Method Development and Results from Beijing, China, *Environmental Science & Technology*, 50(9), 4632-4641, doi:10.1021/acs.est.5b05593, 2016

409  
410  
411  
412  
413  
414  
415  
416  
417  
418  
419  
420  
421  
422  
423  
424  
425  
426  
427  
428  
429  
430  
431  
432  
433

Figure captions

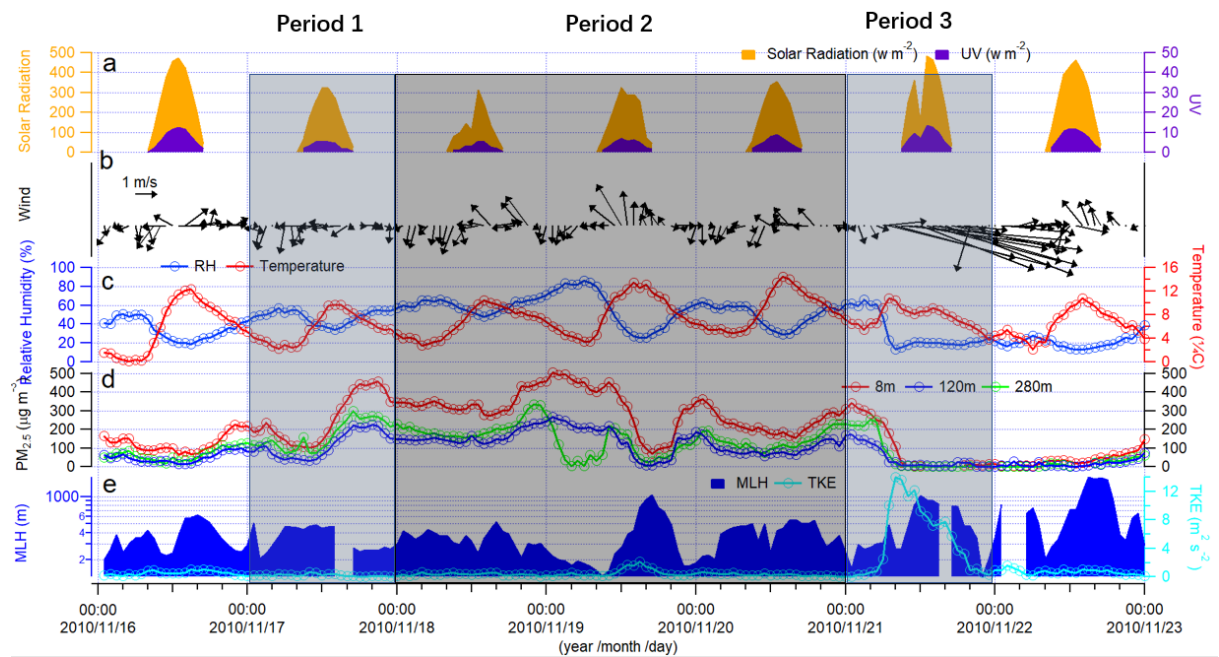


**Figure 1.** Measurements of (a) solar radiation and ultraviolet radiation at 8 m, (b) wind speed and direction at 8 m, (c) relative humidity and air temperature at 8 m, (d) mass concentration of  $\text{PM}_{2.5}$  at 8 m, 120 m and 280 m, (e) mixing layer height at 8 m and turbulence kinetic energy at 140 m in the Beijing 325-meter meteorology tower during an intensive air pollution episode in November of 2010. The evolution of the air pollution episode can be divided into the period 1 (clean period to air pollution accumulation period, period 2 (pollution period) and period 3 (pollution to clean period).

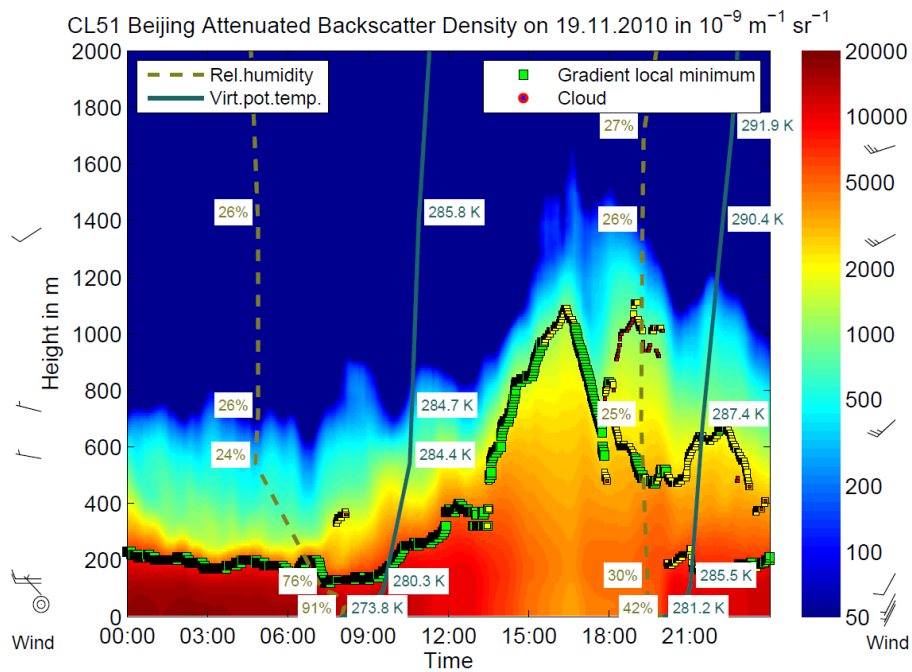
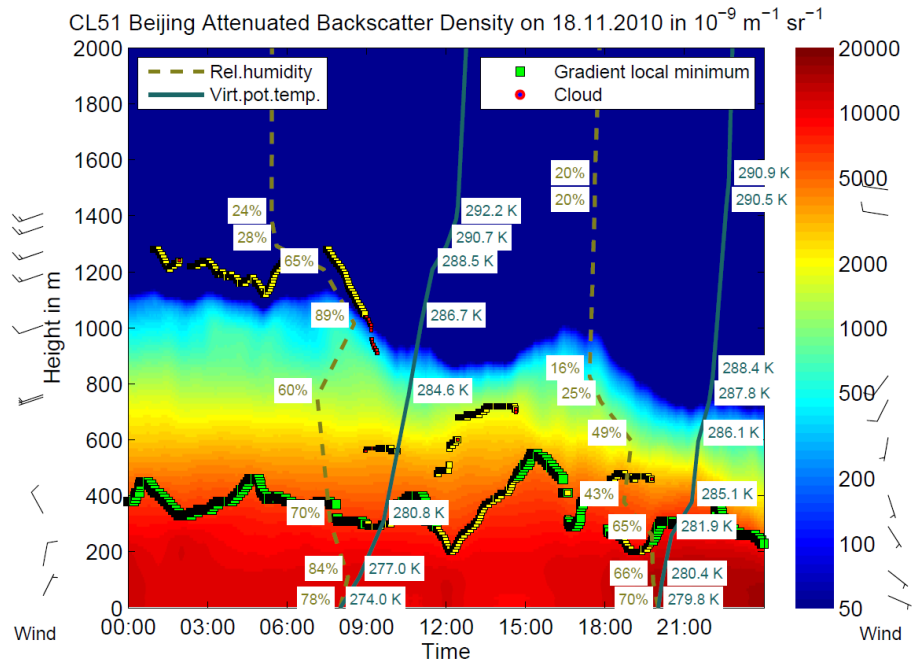
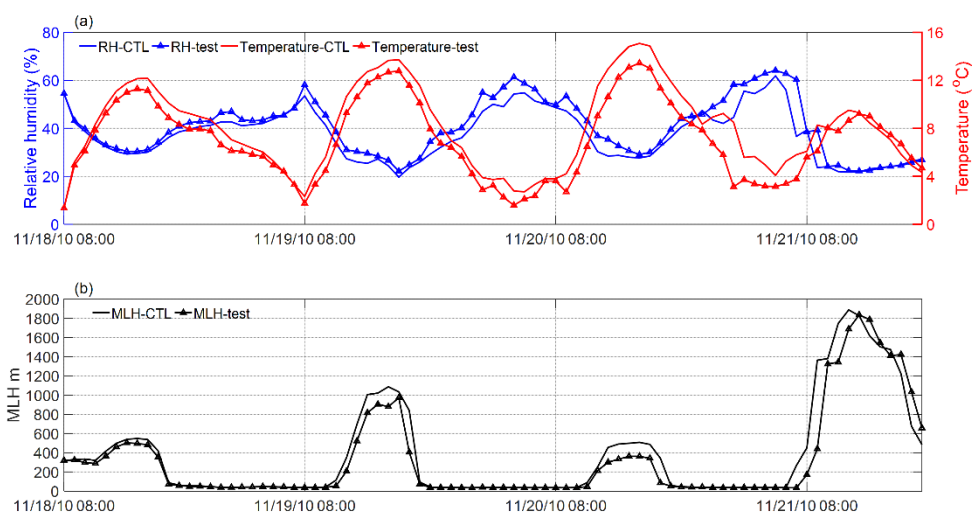


**Figure 2.** Observed attenuated backscatter density, calculated mixing layer height using ceilometer and vertical wind speed, wind direction, relative humidity, virtual potential temperature using sounding data during November 18 (top) and 19 (bottom). The black flag in the left and right side of the figures stand for vertical wind speed and wind direction obtained from sounding measurements at 08:00 and 20:00 of Beijing time, respectively. The circle in the left side of figure represents calm wind. The dotted yellow lines and solid green lines represents vertical distribution of virtual potential temperature and relative humidity from sounding at 08:00 and 20:00,



respectively. The yellow square and green square represent first layer and second layer, respectively, and usually the first layer was used as mixing layer height. The mixing layer height was determined from the local minimum of the backscatter density gradient, and the colour in the figure stands for backscatter density from ceilometer. From both figures, we can clearly see that mixing layer has important role in regulating distribution of air pollutants.

461



462

463 Figure 3(a) Modeled variation of surface relative humidity, temperature and (b) mixing layer height  
464 during the intensive haze episode from 18<sup>th</sup> November 2010 to 21<sup>th</sup> November 2010. The lines with  
465 triangles on represent results from test experiment, while the lines represent results from control  
466 experiment. The control experiment was performed with absence of aerosol direct radiative forcing  
467 in the RRTMG radiation scheme, while the test experiment was conducted with presence of aerosol  
468 direct radiative forcing considered.

469

470

471

472

473

474

475

476

477

478

479

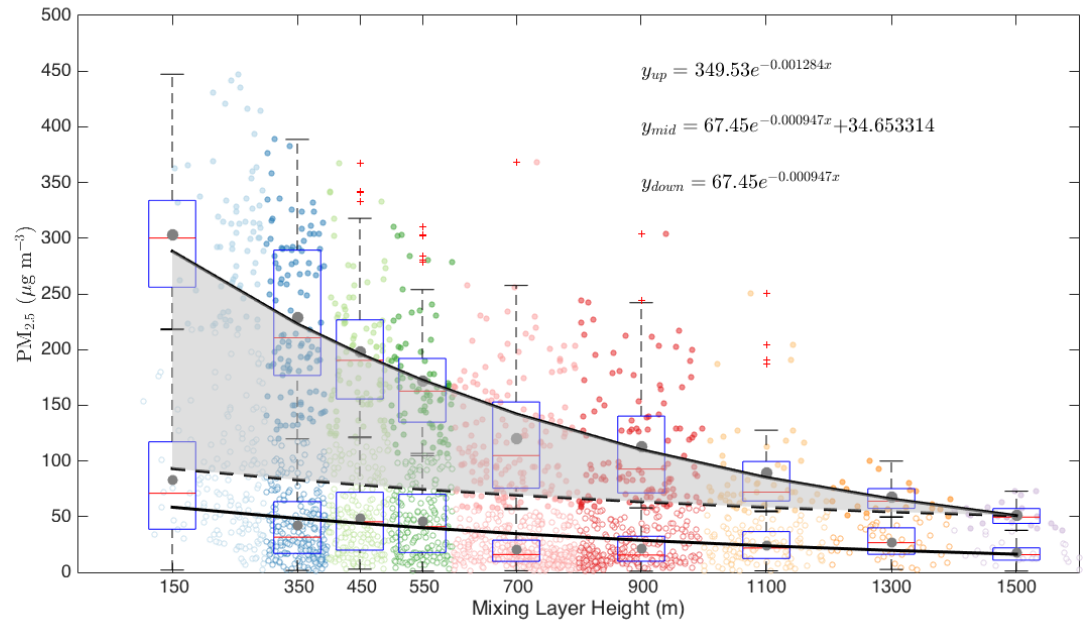
480

481

482

483

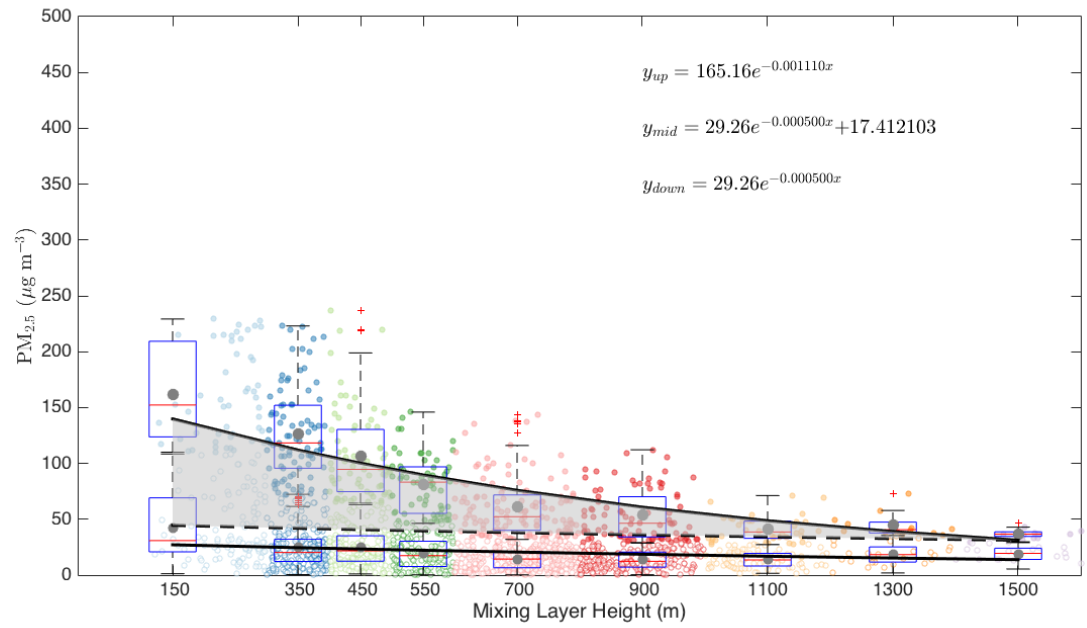
484



485

486

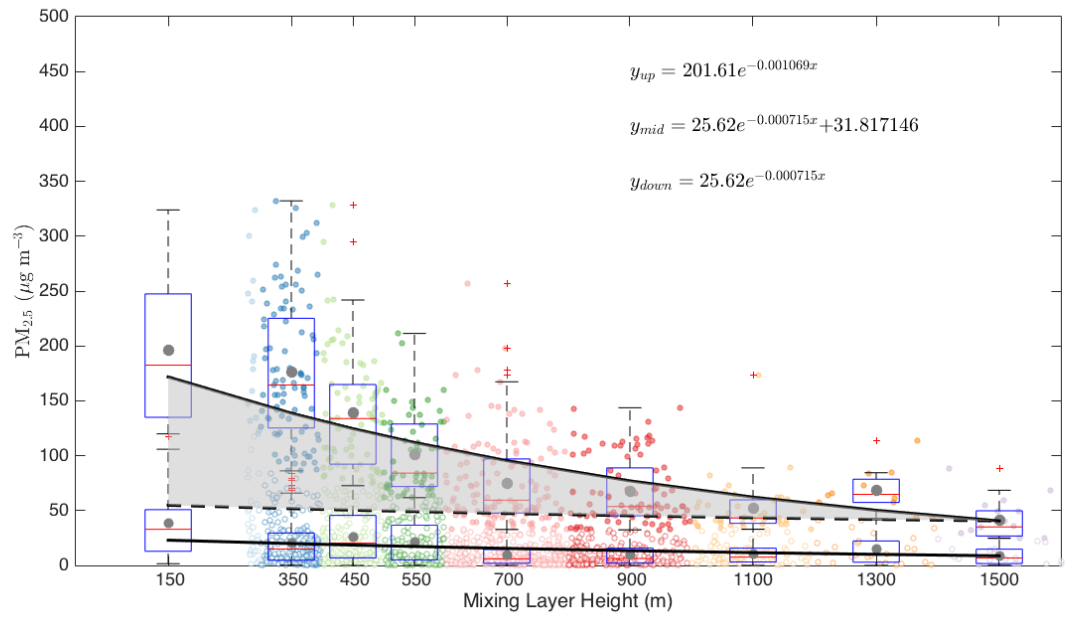
(a)



487

488

(b)



(c)

**Figure 4.** The variability of the PM<sub>2.5</sub> mass concentration as a function of the mixing layer height at 8 m (a), 120 m (b) and 280 m (c). The data related to the upper fitting line represents PM<sub>2.5</sub> concentrations larger than 75 ug m<sup>-3</sup>, while the data related to the lower fitting line represents PM<sub>2.5</sub> concentrations less than 75 ug m<sup>-3</sup>. The dark grey points represent mean values; the red line represents median values. The shadowed area corresponds to an increased amount of PM<sub>2.5</sub> with decreased mixing layer height assuming that PM<sub>2.5</sub> has the same variation pattern under highly- polluted conditions as in less polluted time.

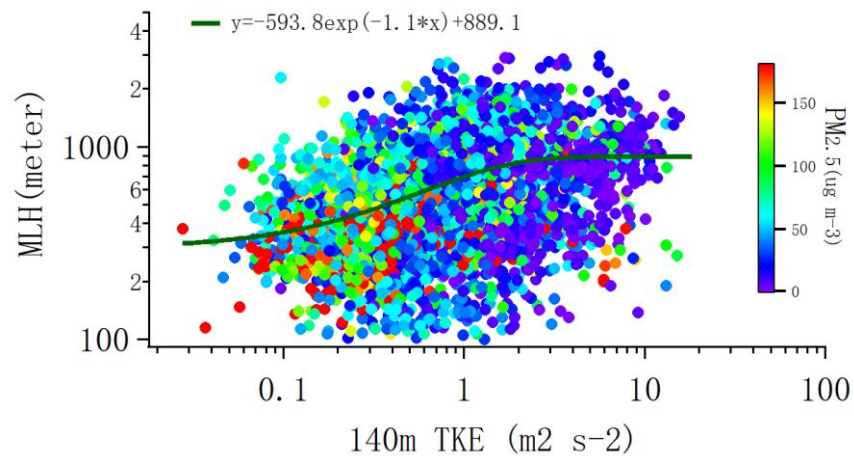


**Figure 5.** Turbulent kinetic energy at 140 m as a function of mixing layer height and PM<sub>2.5</sub> concentrations at 120 m from July of 2009 to August of 2011. An exponential function was fitted based on best fitting.